

# Structural, optical and electrical characteristics of nickel oxide thin films synthesised through chemical processing method

**Shadrach Akinkuade<sup>\*</sup>, Jacqueline Nel and Walter Meyer**

*Physics Department, University of Pretoria, Pretoria 0002, South Africa*

<sup>\*</sup>Corresponding author. E-mail address: [u14302552@tuks.co.za](mailto:u14302552@tuks.co.za), Tel: +27610858343

## **Abstract**

A simple and cheap chemical deposition method was used to produce a nickel oxide (NiO) thin film on glass substrates from a solution that contained Ni<sup>2+</sup> and monoethanolamine. Thermal treatment of the film at temperatures above 350 °C for 1 h caused decomposition of the nickel hydroxide into nickel oxide. Structural, optical and electrical properties of the film were studied using X-ray diffraction (XRD), spectrophotometry, current-voltage measurements and scanning electron microscopy (SEM). The film was found to be polycrystalline with interplanar spacing of 0.241 nm, 0.208 nm and 0.148 nm for (111), (200) and (220) planes respectively, the lattice constant  $a$  was found to be 0.417 nm. The film had a porous surface morphology, formed from a network of nanowalls of average thickness of 66.67 nm and 52.00 nm for as-deposited and annealed films respectively. Transmittance of visible light by the as-deposited film was higher and the absorption edge of the film blue-shifted after annealing. The optical band gap of the annealed film was 3.8 eV. Electrical resistivity of the film was  $3.78 \times 10^4 \Omega\text{cm}$ .

**Keywords** Chemical deposition; NiO; Thin film; Polycrystalline, Optical band gap; Electrical resistivity

## 1. Introduction

Transparent conductive oxides (TCO) such as indium tin oxide (ITO) and zinc oxide are wide bandgap semiconductors; and have been used in many applications such as transparent electrodes, solar cells and touch panels [1]. Nanostructures of various metal oxides have been investigated for hydrogen production [2] and gas sensing. Some of these TCOs which have been studied extensively are n-type semiconductors [3]. In some applications where n-type semiconductors are used, p-type semiconductors are also required to produce complementary devices or for the fabrication of p-n junctions, which are essential for the study of electrical properties and defects in n-type materials like zinc oxide [4], and to enhance the gas sensing properties of metal oxide sensors. Since it is difficult to achieve p-type conductivity by doping in n-type metal oxide semiconductors, research efforts are focused on p-type materials such as nickel oxide. Nickel oxide (NiO) is one of the few metal oxides with p-type properties; it has a stable, wide bandgap of 3.5 to 4.0 eV [7,8], it has been used in electrochromic [7], photoelectrochemical water splitting [8], gas sensing [9] and energy storage [10] applications. It has been reported as having an excellent chemical stability, high optical transparency and electrical conductivity. Different deposition methods such as pulsed laser deposition, dip coating, spin coating, sputtering, spray pyrolysis and chemical bath deposition (CBD) have been used to deposit thin films of nickel oxide. All these methods offer different advantages depending on the specific application of interest [11]. Among the methods, chemical bath deposition has been adjudged to be advantageous due to its relative simplicity, low cost, low temperature, scalability and good control over the deposition process [12]. According to our knowledge, there is no report on electrical characterisation of porous thin films of nickel oxide. In this work, thin films of NiO were produced by the simple and economical chemical bath deposition method. The films were characterized by

scanning electron microscopy (SEM), atomic force microscopy, X-ray diffraction (XRD), UV-Vis spectrophotometry and I-V/C-V measurements.

## **2. Experimental**

### **2.1 Preparation of NiO thin film**

All chemicals were of analytical reagent grade and used without further purification. The substrates were microscope slides cut into 25 mm by 10 mm and ITO coated glass. Prior to deposition, substrates were first soaked in warm detergent solution for 5 minutes, rubbed to remove any grease and rinsed in de-ionized water. They were later washed in an ultrasonic bath at 30 °C for 10 minutes each in de-ionized water, acetone and ethanol and then blow-dried using nitrogen gas. One side of each substrate was covered with tape to avoid deposition on both sides. The chemical bath was formed by adding 0.4 g of polyvinyl alcohol (PVA) into 40 ml of de-ionized water; the solution was stirred at 250 rpm and heated gently to 90 °C. The temperature of the solution was allowed to fall to 30 °C and 0.5257 g of nickel sulphate hexahydrate ( $\text{NiSO}_4 \cdot 6\text{H}_2\text{O}$ ) was added to the solution and stirred until it dissolved completely, where after 3 ml of monoethanolamine (MEA) was added to form a deep blue solution. The pH of the bath taken before deposition was found to be 11.50. Substrates were vertically immersed in the bath which was heated gently. Formation of green precipitates commenced at 60 °C. The bath was maintained at 70 °C for 1 hour while deposition occurred. After 1 hour the solution became green and turbid. Substrates were removed, washed with de-ionized water and dried in an oven at 150 °C for 10 minutes. The pH of the bath after deposition was 11.32. Precipitates formed in the chemical bath were washed four times in de-ionized water, filtered and dried in an oven at 100 °C for 10 minutes and subjected to thermogravimetric analysis (TGA) which was carried out from 17 °C to 1000 °C in Nitrogen at a flow rate of 50.0 ml/min. Films were annealed at different temperatures, between 350 °C,

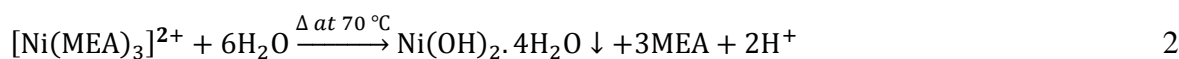
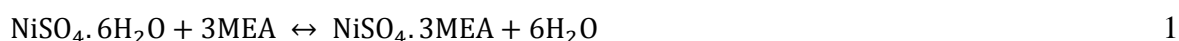
and 500 °C for one hour in air. Aluminium contacts of diameter 0.6 mm and thickness 300 nm were resistively evaporated on the film that was deposited on ITO/glass substrates, after annealing.

## 2.2 Analysis and Characterization of the film

Microstructures of the nickel oxide film were investigated using XRD with Co K $\alpha$  radiation. For the morphological analysis, field emission scanning electron microscopy (FESEM) in a ZEISS Crossbeam 540 at 1 kV acceleration voltage was used. A Jobin Yvon, Horiba<sup>®</sup> TX64000 was used for Raman studies. Optical transmittance and absorbance spectra of the film were obtained in the ultraviolet (UV) and visible region in the wavelength range 200 to 800 nm using a CARY 100 BIO UV-VIS spectrophotometer. The electrical properties of the film between -2 V and 2 V at room temperature and in the dark were measured using I-V measurements with a HP 4140 B pA meter/DC voltage source.

## 3. Results and discussion

Formation of nickel oxide thin film may be described by the following chemical equations:



The first equation involves the formation of a deep blue complex of nickel and monoethanolamine, which had a pH of 11.50. When heated, the complex slowly releases Ni<sup>2+</sup> which in the presence of water at 70 °C, forms hydrated nickel hydroxide on the substrate according to equation 2. The pH of the solution after deposition was found to be 11.32, thus monoethanolamine provides the ideal pH for deposition of NiO in CBD.

According to the TGA results shown in Fig. 1, weight loss in the precipitates occurred in three steps: The first weight loss of 5.67 % took place from 50 °C to 200 °C, this can be attributed to evaporation of water of crystallization. The second and major weight loss (16.36 %) in the range 200 °C to 600 °C, centred on 350 °C is due to thermal decomposition of nickel hydroxide to form nickel oxide according to equation 3. Weight loss at temperatures above 600 °C (5.07 %) was insignificant. Colour of the film changed from green to grey after thermal treatment as shown in the inset of Fig. 1.

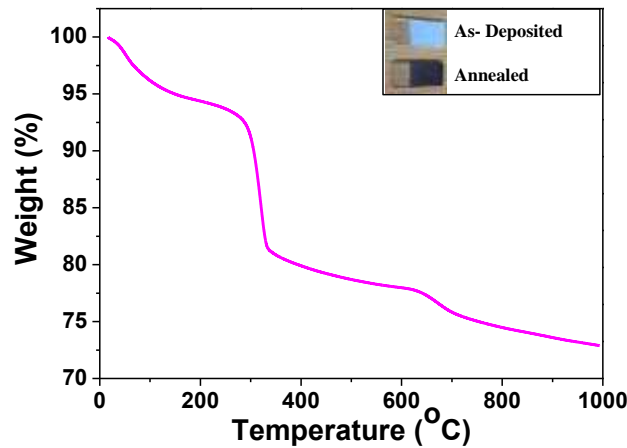


**Fig. 1.** Thermogravimetric curve of the NiO thin film. The inset is the photograph of the as-deposited and annealed film.

The XRD pattern of the film, indexed to JCPDS file No. 04-0835 [15, 16], is shown in Fig. 2. Three peaks at 43.57 °, 50.99 ° and 74.61 ° which were assigned to (111), (200) and (220) peaks of cubic NiO can be seen in the films annealed at 350 °C and 500 °C. The interplanar spacing  $d_{hkl}$  can be calculated from Bragg's law as:

$$d_{hkl} = \frac{\lambda}{2 \sin \theta} \quad 4$$

where  $\lambda$ , the wavelength of Co K $\alpha$  radiation is 1.788965 nm and  $\theta$  is the incident angle at which maximum diffraction occurs. The lattice constant  $a$  was calculated from [14]:

$$a = d_{hkl}\sqrt{(h^2 + k^2 + l^2)}$$

Calculated interplanar spacing and lattice constants are shown in Table 1. The d-spacing and lattice constants were very close to values obtained by [4, 10, 15, 16, 17].

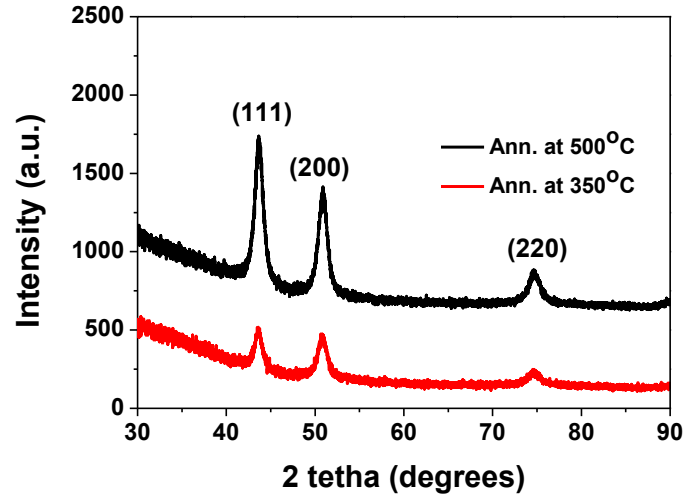


**Fig. 2.** X-ray diffraction (XRD) patterns of the annealed film

**Table 1:** Information from XRD of the annealed film

$(hkl)$	JCPDS no. 04-0835		Calculated for the NiO thin film	
	[14]		$d$ (nm)	lattice constant $a$ (nm)
	$d$ (nm)			
111	0.2410	0.2410	0.4175	
200	0.2088	0.2078	0.4156	
220	0.1476	0.1477	0.4177	

Morphologies of the as-deposited and annealed films are shown in Fig. 3; there was no remarkable difference between these morphologies. The morphology which is porous with many interconnected nanowalls that grow vertically on the substrate forming a honeycomb like structure does not agree with the cubic structure of NiO. However, they are similar to what have been reported by [11] and [16]. The thickness of the nanowalls as measured at indicated points in Fig. 3a and b varied between 66.67 nm to 116 nm in the as-deposited film,

with an average of 76.67 nm. After annealing the films at 450 °C, the thickness varied between 33.33 nm and 58.33 nm with an average of 52.00 nm. Average thickness of the film on glass, as shown in Fig. 3c was 1  $\mu\text{m}$ .

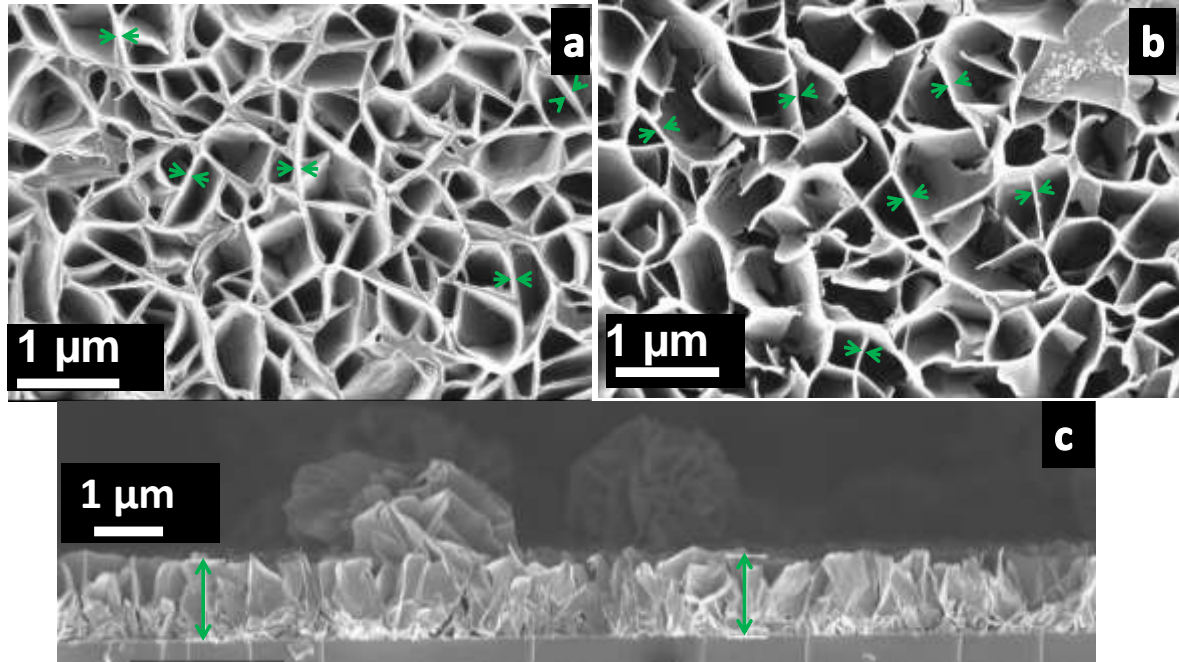


**Fig. 3.** SEM micrographs of NiO thin film (a) as-deposited (b) annealed and (c) cross-sectional image of annealed film.

Raman spectra of the as-deposited and annealed films between 200 and 2000  $\text{cm}^{-1}$  are shown in Fig. 4. Raman shifts at 560  $\text{cm}^{-1}$  and 1100  $\text{cm}^{-1}$  corresponding to one-phonon (1P) LO and two-phonon (2P) LO of vibrational origin similar to what was reported by [17] are seen in the spectra of the annealed film.

Fig. 5 shows the optical transmittance spectra of the annealed film. Transmittance in the visible range (380-750 nm) varied from 8.54 % to 54.28 % for the as-deposited film and 6.67 % to 49.76 % for the annealed film. In the ultraviolet range transmittance decreased; at 325 nm it was 2.27 % and 1.21 % for the as-deposited and the annealed film respectively. This corresponds with an absorption peak of NiO thin film at 320 nm reported in [18]. The

recorded low value of transmittance in the visible range may be due to scattering of light from the interconnected walls in the morphology.

The relation between the absorption coefficient ( $\alpha$ ) and incident photon energy ( $h\nu$ ) can be expressed as [19]:

$$(\alpha h\nu) = A(h\nu - E_g)^n$$

6

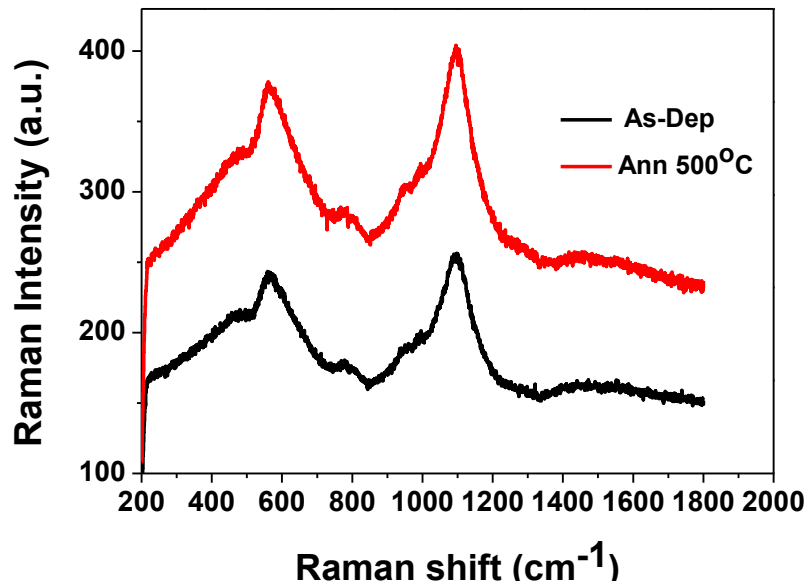


Fig. 4. Raman spectra of NiO thin film

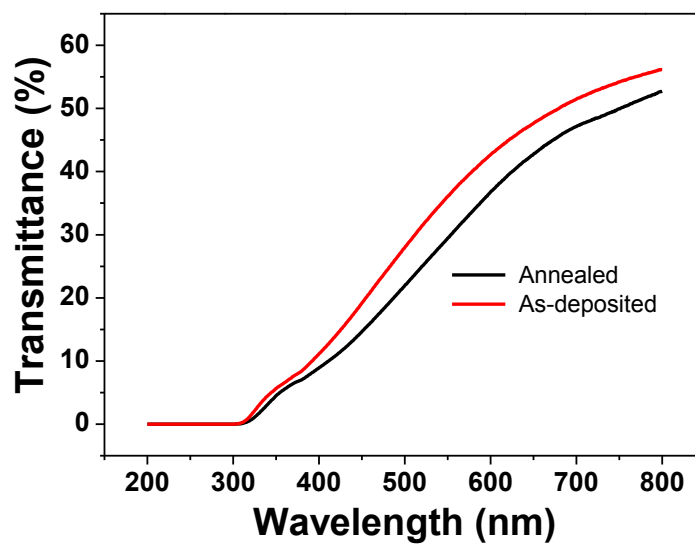


Fig. 5. Transmittance spectra of NiO thin film



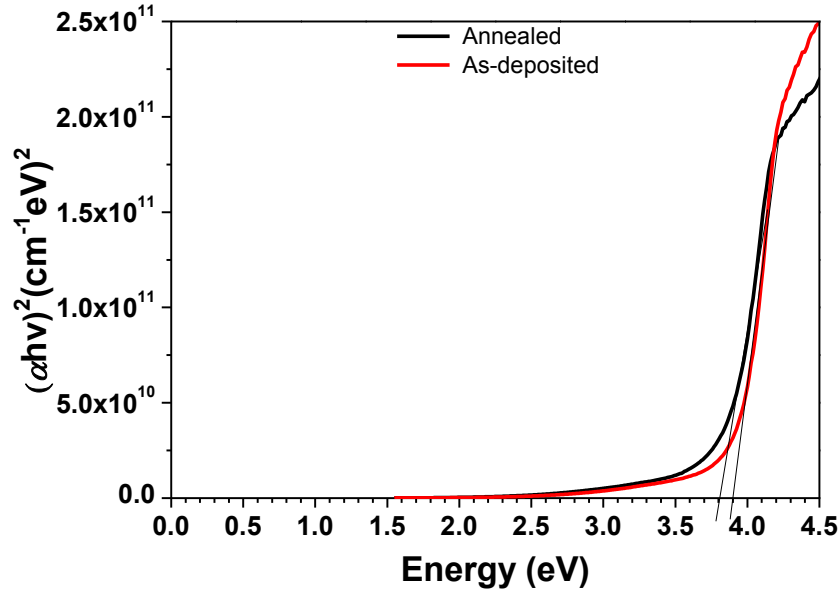


Fig. 6. Tauc Plot of NiO thin film annealed at 450 °C for 1 hr

where  $A$  is a constant,  $E_g$  is the optical band gap of the material and  $n$  is a number which depends on the type of transition involved. For a transition of an electron from the valence to the conduction band of the material, a direct allowed, an indirect allowed, a direct forbidden and an indirect forbidden,  $n$  has values of  $\frac{1}{2}$ ,  $2$ ,  $\frac{3}{2}$  and  $3$  respectively. For NiO, the value of  $n$  is  $\frac{1}{2}$ . A plot of  $(\alpha hv)^2$  versus  $hv$  was plotted as shown in Fig. 6, and the optical band gap of the films, found by extrapolating linear part of the curve to the  $hv$  axis, was 3.9 eV and 3.8 eV for the as-deposited and annealed films respectively; this is within the range reported in literature [7,8].

An aluminium/nickel oxide/ITO structure that was formed by evaporation of aluminium contacts on the film is shown in Fig. 7a, the I-V characteristics of the film are shown in Fig. 7b. Resistance of the film as calculated from the slope of the graph was 1.313 k $\Omega$ ; the electrical resistivity  $\rho$  was obtained from:

$$\rho = \frac{RA}{t},$$

7

where  $R$  is the resistance of the film,  $A$  is the area of the aluminium contact and  $t$  is the film's thickness.

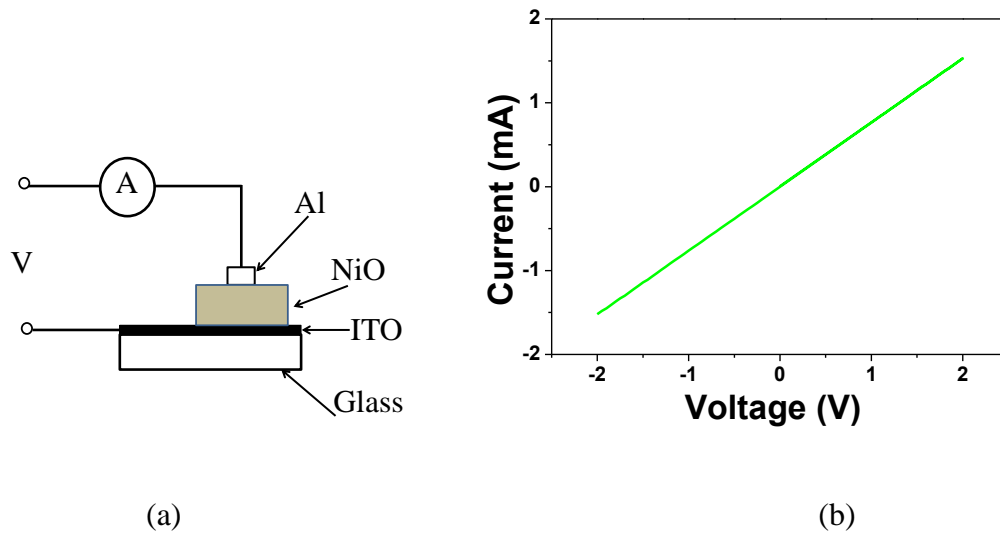


**Fig. 7.** (a) Schematic of Al/NiO/ITO structure used for electrical characterisation (b) I-V Characteristics of NiO thin film.

Considering the morphology of the annealed film, a contact is more likely to cover many nanowalls and pores, more so, during electrical measurement, the exact position of probes on the film cannot be ascertained. Therefore, the resistivity of the film which was found to be  $3.78 \times 10^4 \Omega\text{cm}$  by making use the thickness of the film as shown in Fig. 3c, may be greater than its actual value. Comparison between the properties of the nickel oxide film and others found in literature is shown in table 2.

**Table 2.** Properties of the nickel oxide thin films

Properties			References
Resistivity ( $\Omega\text{cm}$ )	Optical Bandgap (eV)	Nature	
$1 \times 10^4 - 9 \times 10^4$	3.40 – 3.58	Non-porous	[20]
$50 \times 10^3 - 900 \times 10^3$	3.52 – 3.76	Non-porous	[21]
$40 \times -160$	3.49 – 3.75	Non-porous	[21]
$3.78 \times 10^4$	3.80	Porous	This work

#### **4. Conclusions**

A nickel oxide thin film was deposited by means of chemical bath deposition. It had a porous morphology; and there was a decrease in the size of the nanowalls from an average of 76.67 nm to 52.00 nm when the film was subjected to thermal treatment. The film was polycrystalline with lattice constant of 0.417 nm. Optical properties of the film indicate that it was transparent in the visible and near infrared region with maximum transmittance of 49.76 % for the annealed film. However, in the ultraviolet region, transmittance was very low and absorption was high. The absorption edge was blue-shifted with thermal treatment of the film. The optical bandgap of the annealed film was 3.8 eV. The electrical resistivity  $3.78 \times 10^4 \Omega\text{cm}$  in combination with the optical properties, show that these films are not suitable for use as a TCO. However, due to their porosity, they can be used in sensing applications.

#### **Acknowledgements**

This work was financially supported by the University of Pretoria and the National Research Foundation (NRF), South Africa Grant No: 91550. The authors also acknowledge the following: Isbé van der Westhuizen (Institute of Applied Materials), Wiebke Grote (Department of Geology) and Shankara Radhakrishnan (Department of Chemistry); all in University of Pretoria, for the assistance they rendered in carrying out Thermogravimetric, X-ray diffraction and UV-Vis spectrophotometry analyses respectively, of the films.

#### **References**

- [1] W. Chia-ching and Y. Cheng-fu, "Investigation of the properties of nanostructured Li-doped NiO films using the modified spray pyrolysis method," *Nanoscale Res. Lett.*, vol. 8, no. 1, p. 1, 2013.
- [2] A. Qurashi, Z. Zhang, M. Asif, and T. Yamazaki, "Synthesis NiO nanoflowers and

- their photoelectrochemical hydrogen production,” *Int. J. Hydrogen Energy*, vol. 40, no. 45, pp. 15801–15805, 2015.
- [3] L. Cattin, B. A. Reguig, A. Khelil, M. Morsli, K. Benchouk, and J. C. Bernède, “Properties of NiO thin films deposited by chemical spray pyrolysis using different precursor solutions,” *Appl. Surf. Sci.*, vol. 254, no. 18, pp. 5814–5821, 2008.
- [4] F. D. Auret, L. Wu, W. E. Meyer, J. M. Nel, M. J. Legodi, and M. Hayes, “Electrical characterisation of NiO / ZnO structures,” *phys. stat. sol 1*, vol. 677, no. 4, pp. 674–677, 2004.
- [5] L. Berkat, L. Cattin, A. Reguig, M. Regragui, and J. C. Bernede, “Comparison of the physico-chemical properties of NiO thin films deposited by chemical bath deposition and by spray pyrolysis,” *Mater. Chem. Phys.*, vol. 89, no. 1, pp. 11–20, 2005.
- [6] B. A. Reguig, M. Regragui, M. Morsli, A. Khelil, M. Addou, and J. C. Bernède, “Effect of the precursor solution concentration on the NiO thin film properties deposited by spray pyrolysis,” *Sol. Energy Mater. Sol. Cells*, vol. 90, no. 10, pp. 1381–1392, 2006.
- [7] X. H. Xia, J. P. Tu, J. Zhang, X. L. Wang, W. K. Zhang, and H. Huang, “Electrochromic properties of porous NiO thin films prepared by a chemical bath deposition,” vol. 92, pp. 628–633, 2008.
- [8] C. Hu, K. Chu, Y. Zhao, and W. Y. Teoh, “Efficient Photoelectrochemical Water Splitting over Anodized p Type NiO Porous Films,” *ACS Appl. Mater. Interfaces*, vol. 6, pp. 18558–18568, 2014.
- [9] A. A. Khaleed, A. Bello, J. K. Dangbegnon, D. Y. Momodu, M. J. Madito, F. U. Ugbo, A. A. Akande, B. P. Dhonge, F. Barzegar, O. Olaniyan, B. W. Mwakikunga, and N. Manyala, “Effect of activated carbon on the enhancement of CO sensing performance of NiO,” *J. Alloys Compd.*, vol. 694, pp. 155–162, 2017.

- [10] U. M. Patil, R. R. Salunkhe, K. V. Gurav, and C. D. Lokhande, "Chemically deposited nanocrystalline NiO thin films for supercapacitor application," *Appl. Surf. Sci.*, vol. 255, no. 5 PART 2, pp. 2603–2607, 2008.
- [11] M.-G. A. Vidales-Hurtado M.A., "Optical and structural characterization of nickel oxide-based thin films obtained by chemical bath deposition," *Mater. Chem. Phys.*, vol. 107, pp. 33–38, 2008.
- [12] A. M. F. Benial, "Studies on chemical bath deposited CuO thin films for solar cells application," *J. Mater. Sci. Mater. Electron.*, vol. 26, no. 11, pp. 8489–8496, 2015.
- [13] K. H. Kim, C. Takahashi, Y. Abe, and M. Kawamura, "Optik Effects of Cu doping on nickel oxide thin film prepared by sol – gel solution process," *Opt. - Int. J. Light Electron Opt.*, vol. 125, no. 12, pp. 2899–2901, 2014.
- [14] M. S. Yadav and S. K. Tripathi, "Synthesis and characterization of nanocomposite NiO / activated charcoal electrodes for supercapacitor application," *Int. J. Ionics*, 2017.
- [15] S.-Y. Han, D.-H. Lee, Y.-J. Chang, S.-O. Ryu, T.-J. Lee, and C.-H. Chang, "The Growth Mechanism of Nickel Oxide Thin Films by Room-Temperature Chemical Bath Deposition," *J. Electrochem. Soc.*, vol. 153, no. 6, p. C382, 2006.
- [16] J. L. Gunjekar, A. M. More, and C. D. Lokhande, "Chemical deposition of nanocrystalline nickel oxide from urea containing bath and its use in liquefied petroleum gas sensor," vol. 131, pp. 356–361, 2008.
- [17] I. S. and M. P. N. Mironova-Ulmane, A. Kuzmin, I. Steins, J. Grabis, "Raman scattering in nanosized nickel oxide NiO," in *Functional Materials and Nanotechnologies*, 2007, pp. 1–5.
- [18] A. A. Al-ghamdi, W. E. Mahmoud, S. J. Yaghmour, and F. M. Al-marzouki, "Structure and optical properties of nanocrystalline NiO thin film synthesized by sol – gel spin-coating method," vol. 486, pp. 9–13, 2009.

- [19] K. K. Purushothaman, S. J. Antony, and G. Muralidharan, "Optical , structural and electrochromic properties of nickel oxide films produced by sol – gel technique," *Sol. Energy*, vol. 85, no. 5, pp. 978–984, 2011.
- [20] P. S. P. and L. D. Kadam, "Preparation and characterization of spray pyrolyzed nickel oxide ( NiO ) thin films," *Appl. Surf. Sci.*, vol. 199, pp. 211–221, 2002.
- [21] M. Jlassi, I. Sta, M. Hajji, and H. Ezzaouia, "Optical and electrical properties of nickel oxide thin films synthesized by sol – gel spin coating," *Mater. Sci. Semicond. Process.*, vol. 21, pp. 7–13, 2014.